Dynamics of Precursors to Frictional Sliding

S. M. Rubinstein, G. Cohen, and J. Fineberg
Racah Institute of Physics, Hebrew University of Jerusalem, Jerusalem 91904, Israel
(Received 26 March 2007; published 1 June 2007)

We measure the spatial and temporal behavior of the true contact area A along a rough spatially extended interface between two blocks in frictional contact. Upon the application of shear the onset of motion is preceded by a discrete sequence of cracklike precursors, which are initiated at shear levels that are well below the threshold for static friction. These precursors arrest well before traversing the entire interface. They systematically increase in length with the applied shear force and significantly redistribute the true contact area along the interface. Thus, when frictional sliding occurs, the initially uniform contact area along the interface has already evolved to one that is highly nonuniform in space.

DOI: 10.1103/PhysRevLett.98.226103 PACS numbers: 46.55.+d, 46.50.+a, 62.20.Mk, 81.40.Pq

Frictional motion is often conceptually viewed as two rigid bodies sliding on one another. Motion along the interface is traditionally not expected for applied shear forces, $F_S < \mu_S F_N$, where μ_S is the static friction coefficient and F_N the normal force applied. In dry friction, these two bodies are separated by a rough interface, composed of myriad interconnecting microscopic contacts (microcontacts) that bear the entire applied macroscopic load. The true area (sometimes referred to as ''fractional contact area'') $A(x, y, t)$, formed by these contacts, is a key quantity [1,2] as it determines the local resistance to shear at each spatial (x, y) location. For sliding to initiate, these contacts must be fractured. The details of this fracture process are generally not considered in friction, since fracture occurs at speeds approaching material sound speeds, whereas time scales in frictional motion are assumed to be governed by sliding velocities that are orders of magnitude slower. Recent studies, however, have shown that fracturelike [3–5] processes may play a key role at the onset of sliding. In fact, the predictability of material failure under shear [6,7] may well be linked to such rapid precursor events.

The spatial distribution of microcontacts along an interface is often considered to be statistically uniform [2,8], but this assumption is not necessarily warranted in interfaces of large spatial extent. While there is an ongoing debate on how contact area nonuniformity arises, nonuniform microcontact distributions are directly relevant to frictional failure processes including earthquake nucleation and arrest [7,9–13] as well as stick slip in frictional sliding [14].

By measuring the detailed spatial and temporal behavior of A, we show that contact area nonuniformity may arise dynamically via a series of rapid cracklike precursors that propagate partially through the interface. These precursors occur at imposed shears that are well below $\mu_S F_N$ and generate large and systematic nonuniformities of A that precondition the interface well prior to the sliding threshold. The last precursor triggers the transition to sliding by generating a slow front [3] that propagates across the interface.

We performed real-time measurements of the evolution of $A(x, y, t)$ while applying a fixed normal force F_N and slowly increasing F_S. The interface described by $A(x, y, t)$ separates two PMMA (polymethyl-methacrylate) blocks whose contact surfaces were first polished to optical flatness and then lapped to a 1 μm rms surface roughness. The lower block (''base'') had (x, y, z) dimensions of $(300, 30, 27)$ mm with upper blocks (''sliders'') of sizes $(140, 6, 75)$ mm and $(200, 6, 75)$ mm. Here x, y, and z are, respectively, the propagation, sample width, and normal loading directions. Unless otherwise noted, F_S was applied to one edge (the ''trailing'' edge) of the slider at a height $h = 6$ mm above the interface. The contact area was illuminated by a laser sheet, with an incident angle well beyond the angle for total internal reflection from the interface. The light intensity transmitted across the interface, which is proportional to $A(x, y, t)$, was imaged at rates up to 100 000 frames/sec. As the onset dynamics are governed by 1D fronts [3], $A(x, y, t)$ is averaged in the y direction, yielding $A(x, t)$ to 1280 pixel resolution. $A(x)$ was uniform along the interface at the initiation of each experiment. Details of the experimental system are described in [3,15].

A typical experiment is presented in Fig. 1. F_S is slowly increased until the system becomes unstable. Beyond this peak stress, stick-slip-type sliding is initiated, which generates the large subsequent stress drops in Fig. 1(a). A closer look at Fig. 1(a) reveals that, well before sliding, a sequence of small drops in F_S occurs, where the stress released is an order of magnitude less than that released by sliding. As shown in Fig. 1(b), these stress drops correspond to a series of discrete precursor events that are initiated at the sample's trailing edge (where F_S is applied). The precursors extend over well-defined lengths l that are much smaller than the overall length L of the interface. Defining ''sliding'' as motion along the entire interface and ''slip'' as differential motion along parts of the interface, we note that the small stress drops correspond to 3–5 μm slips of the sample's trailing edge ($x = 0$), while the leading edge (at $x = L$) remains pinned.

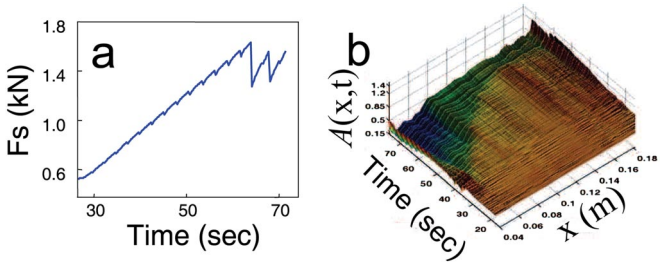

FIG. 1 (color online). The main event triggering sliding is preceded by a sequence of frustrated cracklike precursors. (a) F_S, as a function of time, for a 200 mm long interface loaded at $F_N = 3.3$ kN. (b) The contact area $A(x, t)$ as a function of time and position for the experiment described in (a). $A(x, t)$ is normalized with respect to its spatially uniform value $A(x, t = 0)$ at the start of the experiment. The discrete events noticeable in (a) are manifested as bright ridges in the figure. Each value of $A(x, t)$ is smoothed over 10 mm.

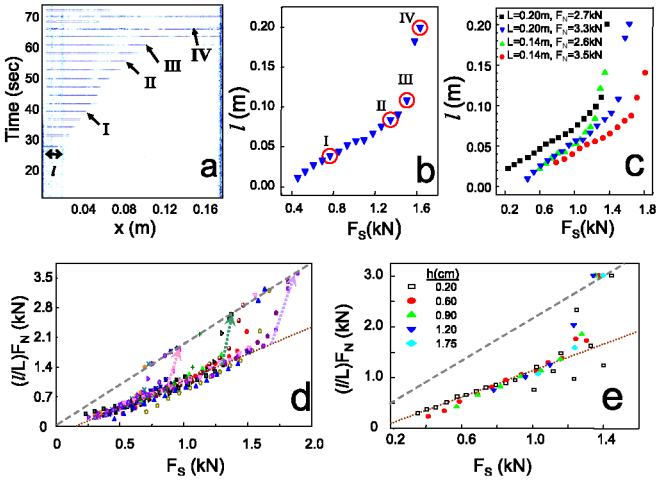

FIG. 2 (color online). Precursors are discrete cracklike events that initiate at the sample's trailing edge. (a) The temporal derivative $|dA(x, t)/dt|$ at each x location [for the experiment shown in Fig. 1(b)], whose intensity is proportional to $|dA(x, t)/dt|$. (b) l as a function of F_S (a). Three precursor events, I, II, and III, and the main sliding event, IV, are marked. Measurement error is approximately the symbol size. (c) l vs F_S in four typical experiments. (d) Twenty-three experiments with $1200 < F_N < 4000$ N and $L = 0.14$ and 0.2 m exhibit data collapse when F_N is scaled by (l/L). Arrows mark the transition to sliding and the breakdown of scaling in 3 typical cases. When sliding, $l = L$ and the Coulomb-Amontons law is realized (dashed line). (e) F_N [scaled as in (c)] as a function of F_S for different values of the height h of the applied shear force above the interface for $L = 0.14$ m.

The precursor events generate significant changes in the contact area. The time derivative, $|dA/dt|$, of the data in Fig. 1(b), presented in Fig. 2(a), demonstrates that the largest changes in A (dark colors) occur during the short (millisecond scale) propagation time of these precursor events.

Figures 2(b) and 2(c) demonstrate that l grows approximately linearly with F_S until rapid growth occurs at $l \sim L/2$ that culminates with sliding at $l = L$. Although the $l - F_S$ curves have a qualitatively similar appearance, their dependence on both L and F_N is evident. Data collapse of $l - F_S$ curves in the linear region is obtained when F_N is scaled by l/L. This is demonstrated in Fig. 2(d), where the linear regions of 23 different experiments, performed with different F_N and L values, collapse onto a single curve. This simple scaling of F_S can be understood by considering how stress is transferred along the interface. F_S is applied at the sample's trailing edge. Because the interface is pinned, shear stress rapidly decays with the distance from the loading point. As F_S is increased, however, the stress σ_S builds up and can only be relieved by slip at the interface. Slip redistributes the stress along the precursor length, yielding a mean stress of $\sigma_S \sim F_S/l$. This scenario suggests a "local" generalization of the Amontons-Coulomb law ($\sigma_S = \mu_S \sigma_N$) where $\sigma_S \sim F_S/l \propto F_N/L \sim \sigma_N$, which is indeed the scaling observed. Significantly, this scaling is not consistent with a simple Griffith-type criterion (i.e., $\sigma_S l^{1/2} \sim$ const) for the onset of shear fracture [16].

These arguments predict that the above scaling should be independent of the details of the loading, as long as F_S is applied at the trailing edge. To check this, we systematically varied h, the height at which F_S is applied, above the interface. We indeed find that the $F_S \propto F_N l/L$ scaling is unchanged [Fig. 2(e)] although both the initial precursor lengths and successive increments of l *do* scale with h. This suggests that, as long as the interface is pinned, the imposed shear only effectively extends over a range h from the point of application. Once the first precursor is excited, it relieves this excess stress and hence arrests after traversing a distance $l \propto h$. This process repeats itself [leading to the rough periodicity in Fig. 1(a)] with each successive precursor triggered at a constant increment of F_S. In this picture, the transfer of stress (hence slip) across the interface is a "leapfrogging" process rather than a slow diffusive one.

The $F_N l/L$ scaling breaks down when l approaches L. As evident in Fig. 2(d), the scaled $l - F_S$ curves diverge from linearity at $l/L = 0.52 \pm 0.04$ and signal the transition towards sliding [arrows in Fig. 2(d)]. As L was varied while keeping the base and other slider dimensions fixed, the transition to sliding at a constant l/L value indicates that this threshold is not influenced by the location of the boundaries normal to the sliding direction. The dashed line in Fig. 2(d), whose slope is $1/\mu_s$, is simply the Amontons-Coulomb law of friction that is obtained when sliding occurs for $l = L$.

How does the transition to sliding occur? Until now we have described the system's evolution at time scales (seconds) that are characteristic of the overall loading rates. Previous work [3] has shown that, at millisecond time scales prior to the onset of sliding, three different types

of detachment fronts play a role: sub-Rayleigh, intersonic [5], and slow detachment fronts. Let us consider the precursors marked I, II, and III in Fig. 2 and the resulting sliding, marked as IV. Figure 3 presents measurements of $A(x, t)$ at 14 μ sec intervals that bracket each of these events. All events are initiated at the trailing edge by "sub-Rayleigh" fronts, propagating at velocities of the order of the Rayleigh wave speed (940 m/sec), which arrest abruptly at a distance l from the trailing edge. In all of the precursors within the scaling regime (e.g., I and II in Fig. 3) the entire event is characterized by the propagation and arrest of a single sub-Rayleigh front. In contrast, the breakdown of scaling in the l vs F_S curves is accompanied by a different scenario. Here, the transition region to sliding (as highlighted in Fig. 3, event III) is accompanied by a slow (20–50 m/sec) detachment front which is triggered by the arrest of the sub-Rayleigh front. In the transition region [denoted by the arrows in Fig. 2(d)] the slow fronts do not traverse the entire interface, but arrest. As in [3], sliding occurs when a slow front either continues to the end of the sample or triggers an additional sub-Rayleigh front that reaches the leading edge. Figure 3 (IV) is an example of the latter case. This slow front is triggered at the same value of l as the preceding events within the transition region.

Perhaps the most important consequence of the precursor dynamics is the evolution of the contact surface generated by these events. As demonstrated in Fig. 1(b), by the time the system is ready to slide, the precursor sequence has significantly altered the contact area profile $A(x, t)$. Hence, the main event propagates into a highly nonuniform interface. In Fig. 4(a) we present a succession of typical $A(x, t)$ profiles, starting from the first precursor to immediately prior to sliding. Starting from a uniform profile at $F_S = 0$, each precursor systematically increases the contact area in the regions adjacent to the leading and trailing edges of the sample, while progressively decreasing $A(x)$ within the interior regions. The length of the reduced contact area region roughly follows the precursor length l. Beyond slow changes precipitated by aging [1], no significant changes to $A(x)$ occur between precursor events. It is surprising that [see inset of Fig. 4(a)], upon sliding, the spatial profile of $A(x)$ is *not* renewed, but is virtually unchanged upon successive sliding-arrest sequences in the ensuing "slip-stick" motion. $A(x)$ only regains uniformity if F_N is fully reduced.

The large local changes in $A(x)$ are quantified in Fig. 4(b), where we compare the peak-to-peak values of $A(x)$ with its mean value as time evolves. While the overall contact area is only decreased by about 10% by the precursor sequence, the peak-to-peak contact area values ΔA change drastically. By the onset of sliding, the interface cannot be considered as at all flat, with ΔA comparable to the mean contact area.

The magnitude of the redistribution of A is surprising. This is much larger than the roughly 10% overall changes in A resulting from aging and renewal [11,17] of contacts due to slip. In addition, models of friction [11,17] tacitly assume that every slip event will renew A to a spatially uniform initial level corresponding to a "fresh" interface. Instead, we have shown that something entirely different happens. First, after each successive precursor (slip event) the surface area becomes systematically less uniform. Thus, in the above sense, surface renewal does not occur

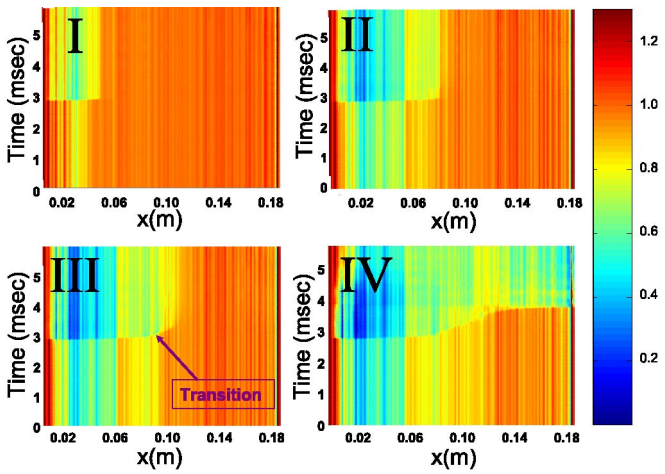

FIG. 3 (color online). The transition to sliding is precipitated by a slow detachment front. Plotted is the short-time temporal evolution of $A(x, t)$, normalized [as in Fig. 1(b)] by $A(x)$ at $F_S = 0$, at intervals of 14 μs for 4 different precursors. The four plots correspond to the 6 msec bracketing the precursors marked I, II, III and event IV in Fig. 2.

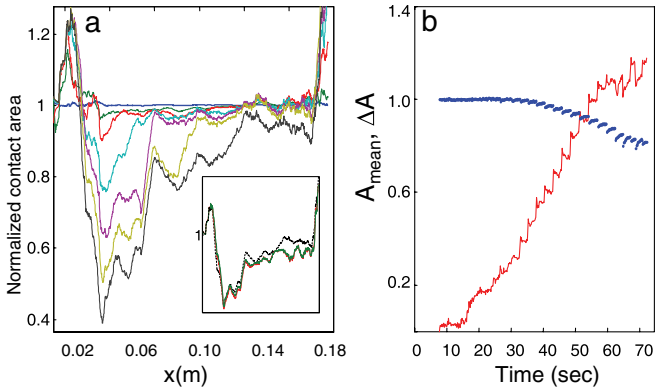

FIG. 4 (color online). The discrete precursor sequences significantly alter the contact area profile. (a) $A(x, t)$ profiles subsequent to every third precursor presented in Fig. 2(a). (Inset) Three $A(x, t)$ profiles, one taken immediately prior to sliding (dotted line) and two immediately following sliding in consecutive stick-slip events of approximately 50 μm, show that $A(x)$ profiles are not modified during successive slip-stick events. (b) A comparison between the (bold line) mean contact area A_{mean} and (thin line) the peak-to-peak amplitude, $\Delta A = A(x, t)_{\max} - A(x, t)_{\min}$, characterizing the nonuniformity of $A(x)$. All $A(x)$ curves were smoothed over 10 mm.

at all. Second, the cumulative effect of the precursors can generate values of ΔA that are an order of magnitude larger than expected. Finally, sliding causes virtually negligible changes in the surface contact profile, providing an explanation for the empirically well-known observation that the first sliding event is qualitatively different than successive stick-slip events. The above results suggest that nonuniformity of $A(x)$ is, in some sense, the preferred state of the system during sliding. It is important to note that the excitation of cracklike precursors to sliding which, upon their passage, significantly modify the contact area, generally occurs and is not limited to the specific type of loading presented here. Upon the application of uniform shear (when the scaling in Fig. 2 does *not* occur) these effects are still observed.

The scaling behavior of the precursors *does* result from the type of loading applied. This is a classic loading configuration, which is used in numerous studies of friction [9,14,17]. Let us now consider the applicability of these results to the dynamics of earthquakes. Whereas it is generally assumed that a geophysical fault is remotely loaded by uniform shear, either nonuniformity surrounding a fault or an obstacle near an earthquake hypocenter may effectively lead to a section of the fault that undergoes accentuated shear loading at one of its edges. Our results suggest that in such cases we might expect a sequence of small periodic earthquakes of slightly (h dependent) increasing magnitude that initiate at approximately the same hypocenter. This scenario indeed occurs in the well-known sequence of earthquakes near Parkfield, CA [18]. Small tremors coincident with slow, aseismic transients, reminiscent of the precursors and slow fronts in our work, have also recently been observed [19] in a region of transient slip within the Nankai trough. In both of these examples the loading is analogous to that in our experiments, as the active regions of transient slip are sandwiched between locked and steadily slipping zones [18,19].

Examination of the qualitative differences between precursors and sliding events may provide additional insights in the context of earthquake dynamics. The transition from arrested sub-Rayleigh precursors to sliding via the generation of slow fronts (Fig. 3) may, for example, imply that large earthquakes qualitatively differ from small ones (precursors) [20]. Here, we associate large earthquakes with sliding over a large (perhaps detached) segment of a fault that is analogous to the system size in our experiments. The same results may also be analogous to the dynamics of earthquake nucleation [9], where precursors trigger a slowly nucleating rupture (the slow front) whose propagation culminates in an earthquake (sliding in our system). The ambiguity of these interpretations stems from the important (and still open) question of how to scale the system size to scales that are applicable to fault dynamics.

We thank M. Robbins for sharing his many insights with us. The authors acknowledge the support of the Israel Science Foundation (FIRST Grant No. 1116/05).

[1] J. H. Dieterich and B. D. Kilgore, Pure Appl. Geophys. **143**, 283 (1994).
[2] F. P. Bowden and D. Tabor, *The Friction and Lubrication of Solids* (Oxford University Press, New York, 2001), 2nd ed.
[3] S. M. Rubinstein, G. Cohen, and J. Fineberg, Nature (London) **430**, 1005 (2004).
[4] E. Gerde and M. Marder, Nature (London) **413**, 285 (2001); K. W. Xia, A. J. Rosakis, and H. Kanamori, Science **303**, 1859 (2004); T. Baumberger, C. Caroli, and O. Ronsin, Phys. Rev. Lett. **88**, 075509 (2002); Y. Ben-Zion, J. Mech. Phys. Solids **49**, 2209 (2001).
[5] Xia, A. J. Rosakis, and H. Kanamori, Science **303**, 1859 (2004).
[6] A. S. Argon and M. J. Demkowicz, Philos. Mag. **86**, 4153 (2006).
[7] B. D. Thompson, R. P. Young, and D. A. Lockner, Geophys. Res. Lett. **32**, L10304 (2005).
[8] M. Urbakh, J. Klafter, D. Gourdon, and J. Israelachvili, Nature (London) **430**, 525 (2004); B. N. J. Persson, *Sliding Friction Physical Principles and Applications* (Springer-Verlag, New York, 2000), 2nd ed.; B. Q. Luan and M. O. Robbins, Nature (London) **435**, 929 (2005).
[9] M. Ohnaka and L. F. Shen, J. Geophys. Res. **104**, 817 (1999).
[10] J. H. Dieterich, Tectonophysics **211**, 115 (1992).
[11] N. Lapusta and J. R. Rice, J. Geophys. Res. **108**, 2205 (2003).
[12] N. Lapusta, J. R. Rice, Y. Ben-Zion, and G. T. Zheng, J. Geophys. Res. **105**, 23 765 (2000).
[13] M. Ohnaka, Pure Appl. Geophys. **161**, 1915 (2004).
[14] S. L. Ma and C. R. He, Tectonophysics **337**, 135 (2001).
[15] S. M. Rubinstein, M. Shay, G. Cohen, and J. Fineberg, Int. J. Fract. **140**, 201 (2006).
[16] E. A. Brener, S. V. Malinin, and V. I. Marchenko, Eur. Phys. J. E **17**, 101 (2005).
[17] J. H. Dieterich, Pure Appl. Geophys. **116**, 790 (1978); P. Berthoud, T. Baumberger, C. G'Sell, and J. M. Hiver, Phys. Rev. B **59**, 14 313 (1999).
[18] C. H. Scholz, *The Mechanics of Earthquakes and Faulting* (Cambridge University Press, Cambridge, 2002).
[19] D. R. Shelly, G. C. Beroza, S. Ide, and S. Nakamula, Nature (London) **442**, 188 (2006).
[20] B. E. Shaw and C. H. Scholz, Geophys. Res. Lett. **28**, 2995 (2001); B. Romanowicz and L. J. Ruff, Geophys. Res. Lett. **29**, 1604 (2002).